Review of Scientific Instruments

Using multiple neutron time of flight detectors to determine the hot spot velocity

Cite as: Rev. Sci. Instrum. **89**, 101138 (2018); https://doi.org/10.1063/1.5039372
Submitted: 07 May 2018 . Accepted: 11 June 2018 . Published Online: 17 October 2018

R. Hatarik, R. C. Nora, B. K. Spears, M. J. Eckart, G. P. Grim, E. P. Hartouni, A. S. Moore, and D. J. Schlossberg

View Online Export Citation CrossMark

ARTICLES YOU MAY BE INTERESTED IN

A fused silica Cherenkov radiator for high precision time-of-flight measurement of DT γ and neutron spectra (invited)
Review of Scientific Instruments **89**, 101120 (2018); https://doi.org/10.1063/1.5039322

Uncertainty analysis of response functions and γ-backgrounds on T_{ion} and t_0 measurements from Cherenkov neutron detectors at the National Ignition Facility (NIF)
Review of Scientific Instruments **89**, 101140 (2018); https://doi.org/10.1063/1.5038816

Calibration of a neutron time-of-flight detector with a rapid instrument response function for measurements of bulk fluid motion on OMEGA
Review of Scientific Instruments **89**, 101131 (2018); https://doi.org/10.1063/1.5037324

NEW AVS Quantum Science
A high impact interdisciplinary journal for ALL quantum science
ACCEPTING SUBMISSIONS

© 2018 Author(s).

Using multiple neutron time of flight detectors to determine the hot spot velocity

R. Hatarik,[a] R. C. Nora, B. K. Spears, M. J. Eckart, G. P. Grim, E. P. Hartouni, A. S. Moore, and D. J. Schlossberg
Lawrence Livermore National Laboratory, Livermore, California 94550, USA

(Presented 17 April 2018; received 7 May 2018; accepted 11 June 2018; published online 17 October 2018)

An important diagnostic value of a shot at the National Ignition Facility is the resultant center-of-mass motion of the imploding capsule. This residual velocity reduces the efficiency of converting laser energy into plasma temperature. A new analysis method extracts the effective hot spot motion by using information from multiple neutron time-of-flight (nToF) lines-of-sight (LoSs). This technique fits a near Gaussian spectrum to the nToF scope traces and overcomes reliance on models to relate the plasma temperature to the mean energy of the emitted neutrons. This method requires having at least four nToF LoSs. The results of this analysis will be compared to an approach where each LoS is analyzed separately and a model is used to infer the mean energy of the emitted neutrons. *Published by AIP Publishing.* https://doi.org/10.1063/1.5039372

I. INTRODUCTION

Inertial Confinement Fusion (ICF) experiments at the National Ignition Facility (NIF) use 192 lasers to compress a fuel capsule containing deuterium (D) and tritium (T) using an indirect drive where the beams shine into a high Z hohlraum.[1,2] Interaction of the lasers with the high-Z material creates a radiation bath that ablates the outer region of a small target capsule, causing the target to be compressed with an implosion velocity in the order of ≈300 km/s.[3] Small asymmetries in the implosion process which can be caused by either an imbalance in the laser drive or due to imperfections in the capsule can cause a significant P1 perturbation in which the hot spot can move at speeds in excess of 100 km/s. The resulting kinetic energy of the hot spot equates to a loss of its thermal energy. Diagnosing this form of drive inefficiency is therefore important to evaluate the performance of each shot.

Neutron time-of-flight (nToF) detectors have long been used at the NIF[4] to determine the neutron yield, the variance of the neutron peak, and the ratio of down-scattered neutrons. If the absolute timing of an nToF detector is known, the position of the peak can be used to diagnose a moving hot spot. One important quantity that has to be known in order to convert the peak position of an nToF scope trace into a projection of the hot spot velocity along its line-of-sight (LoS) is the mean energy of the emitted neutrons. This mean energy depends on the average energy the reacting deuteron and triton have in their center-of-mass frame and has therefore a non-negligible dependence on the local plasma temperature. The mean energy for all neutrons observed by the nToF detector should thus depend on the average temperature of all reacting ions. The work presented in this paper compares two different approaches to correct for this effect: using the model described by Ballabio *et al.*[5] to correct for the energy shift on each LoS separately or using four nToF LoSs together in order to infer the mean energy of the emitted neutrons. In the latter case, the mean energy can also be used to infer a "temperature" by inverting the model from the study of Ballabio *et al.*

II. EXPERIMENTAL SETUP

At the NIF, angular directions are given in a combination of longitudinal (θ = 0°–180°) and latitudinal (ϕ = 0°–360°) angles. There are four identical nToF diagnostic setups; two near the poles and two near the equatorial plane (see Fig. 1). All setups are at a distance approximately 20 m from the target chamber center (TCC). Each system consists of a bibenzyl scintillation crystal, with four photo detectors looking at the crystal through hollow reflective tubes which act as a light guide. These systems are described in detail in Ref. 6. Using four different detectors allows a large dynamic range to be covered since three detectors are photo multiplier tubes with different gains and one is a photo diode. A recent modification to these detectors was to install an additional fused silica rod behind these detectors[7] which acts as a Cherenkov detector to both neutron and γ-radiation. Due to limited data acquisition channels, one of the PMTs had to be decommissioned in order to record the signal of the Cherenkov detectors. This work focuses only on the analysis of the photodiode coupled to the bibenzyl scintillator since the analysis of the Cherenkov detector signal depends on accurately understanding its background.[8]

III. FITTING nToF DATA

The analysis of the nToF data is done by using a parameterized model for the birth spectrum and adding all instrumental

Note: Paper published as part of the Proceedings of the 22nd Topical Conference on High-Temperature Plasma Diagnostics, San Diego, California, April 2018.

[a]hatarik1@llnl.gov

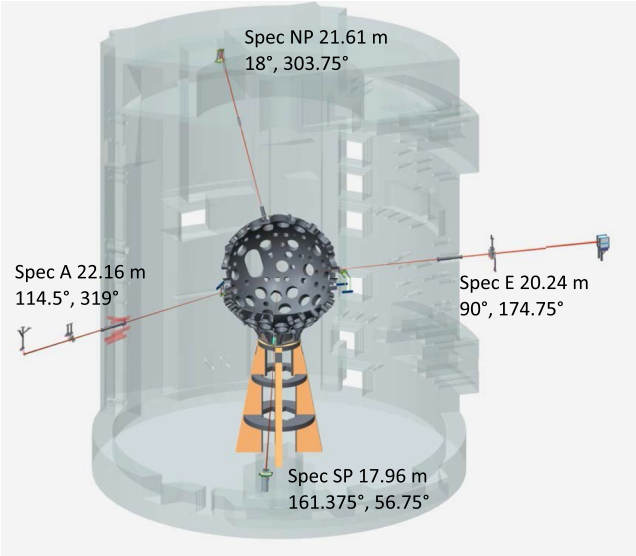

FIG. 1. Location of the four nToF detectors relative to the NIF target chamber.

effects and then fitting the model directly to the scope traces. The fit function takes the following form:

$$f(t) = I(E(t-t_0))s(E(t-t_0))a(E(t-t_0))\frac{dE}{dt} \otimes R(t). \quad (1)$$

Here $I(E)$ denotes the model of the neutron spectrum, $s(E)$ is the sensitivity of the detector to the given neutron energy, $a(E)$ is the beam line attenuation factor, $E(t-t_0)$ and $\frac{dE}{dt}$ are used to convert the energy spectrum into the scope time space, $R(t)$ is the instrument response and t_0 is the time offset needed to convert the scope time axis into time-of-flight. The model of the neutron spectrum $I(E)$ is split up into a source I_{src} and scattering term I_{scat} as described in Ref. 9.

To obtain an absolute timing reference, it is necessary to calibrate by using a timing shot. In these shots, the NIF laser hits a gold foil which causes x-ray emission which can be detected by the scintillator. One issue is that these signals are not large enough to be observed on the photo diode. Therefore it is necessary to get the absolute timing for a PMT on a timing shot and then cross calibrate this PMT to the photo diode on a shot that has a yield which gives good signal on both the PMT and the photo diode.

A. Extracting velocity values from individual lines of sight

One method to extract hot spot motion information is to estimate the plasma temperature from the width of the neutron peak and estimate the peak shift as a function of the temperature. The mean energy can then be calculated as

$$\langle E \rangle = E_0 + \Delta E_{th}, \quad (2)$$

with

$$E_0 = \frac{Q(Q/2 + m_\alpha)}{Q + m_\alpha + m_n} \quad (3)$$

being given by the Q-value (Q = energy released in the reaction), and the energy shift is

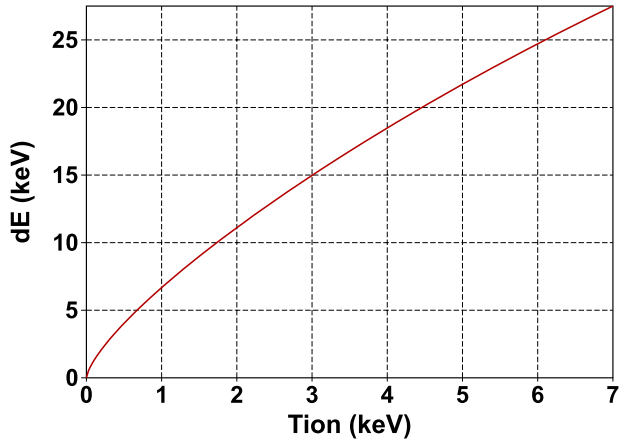

FIG. 2. The energy shift as a function of the ion temperature according to Ballabio *et al.*[5]

$$\Delta E_{th} = \frac{\alpha_1}{1 + \alpha_2 T_{ion}^{\alpha_3}} T_{ion}^{2/3} + \alpha_4 T_{ion}, \quad (4)$$

where the values for $\alpha_1, \ldots, \alpha_4$ are given by Table III in Ref. 5. Figure 2 shows ΔE_{th} as a function of temperature.

While this allows calculation of an energy shift for a given T_{ion}, however, which value to choose for T_{ion} becomes the problem. Since the width of the neutron peak is determined by a quadratic sum of ion temperature and variation in the plasma flow field,[10] the variance of the neutron peak is always larger than if it were determined by temperature alone. For the analysis herein, it was therefore decided to use the lowest temperature determined by the width of the neutron peak on all LoSs. Even though the analysis presented here is only for hot spot velocities from the DT peak, for the purpose of determining the temperature in Eq. (4) the DD temperatures have also been considered for choosing the lowest observed temperature. The method to fit these spectra for the purpose of obtaining values for T_{ion} has been described in detail in Ref. 9.

The velocity can then be extracted by comparing the t_0 fit parameter from Eq. (1) with the reference t_{ref} which is given by

$$t_{ref} = t_{fidu} + t_{lpom} + t_{atten} + t_{bang} + t_{offs}, \quad (5)$$

where t_{offs} is the time offset that needs to be determined from a timing shot, and t_{fidu} stands for the position of the fiducial on the scope trace which is a time marker relative to the system time, while t_{lpom} uses the Laser Performance Operations Model (LPOM) to determine the timing of the NIF laser relative to the system time. t_{atten} corrects the time for any installed electrical attenuators in the signal path, while t_{bang} accounts for the time it takes from the laser hitting the target to the peak burn. Since the scintillator has no way of determining t_{bang}, this time has to be obtained from a different diagnostic such as the Gamma Reaction History (GRH).[11]

If t_{ref} is established, then the projection of the velocity onto the LoS can be calculated using

$$v_{LoS} = d\left(\frac{1}{t_n + t_0 - t_{ref}} - \frac{1}{t_n}\right), \quad (6)$$

where d is the distance from TCC to the detector and t_n is the time a neutron with energy $\langle E \rangle$ would need to travel that distance.

B. Using a multi-line-of-sight analysis

The main disadvantage of analyzing each LoS individually for its velocity projection is its dependence on a model for the mean energy of the neutron peak, especially since it is not really possible to measure ion temperature directly. With the recent addition of a fourth nToF LoS at NIF, an additional option presents itself: determine the mean overall velocity (from mean energy and hot spot motion) v_{LoS} of the neutron peak on all LoSs and reduce the problem to a 4×4 matrix inversion. This assumes that the mean of the overall velocity of the neutron peak can be divided into the sum of two components: the velocity the neutron would have in the reference frame of the hot spot plus the velocity of the hot spot itself. The first part corresponds to $\langle E \rangle$ and is isotropic, i.e., it is the same on all LoSs. The second part comes from the hot spot motion, and each detector sees its projection onto its specific LoS. This can be written as

$$v_{LoS} = \vec{v}_C \cdot \vec{u}_{LoS} + \langle v \rangle \tag{7}$$

with u_{LoS} corresponding to the unity vector pointing along the LoS and $\langle v \rangle$ being the isotropic part originating from $\langle E \rangle$ of Eq. (2). If one defines $\vec{v} = (v_x, v_y, v_z, \langle v \rangle)$ and $\vec{v}_{Los}$ as the vector containing the four LoS velocities, then the problem can be written as the following matrix equation:

$$\vec{v}_{LoS} = M \cdot \vec{v}. \tag{8}$$

Here the matrix M can be expressed as

$$M_{ij} = \begin{cases} \cos\,\phi_i \,\sin\,\theta_i, & j = 1, \\ \sin\,\phi_i \,\sin\,\theta_i, & j = 2, \\ \cos\,\theta_i, & j = 3, \\ 1 & j = 4, \end{cases} \tag{9}$$

with θ_i and ϕ_i being the angles of the ith LoS. Inverting the matrix M allows the calculation of the hot spot velocity vector (v_x, v_y, v_z) and the isotropic component $\langle v \rangle$ which corresponds to the mean velocity of the emitted neutrons in the reference frame of the hot spot. The only assumption needed to determine the velocity vector this way is that all detectors view the same source.

To determine the overall mean velocity on each LoS, the model $I(E)$ in Eq. (1) was changed so that the source term corresponds to a near Gaussian in neutron momentum space. The exact form is given by

$$\begin{aligned} I_{src}(E) &= I_{src}(p)\frac{dp}{dE} = \frac{1}{\beta} I_{src}(p), \\ I_{src}(p) &= \frac{A}{\sqrt{2\pi}\sigma}\left[He_0(x) + \frac{\gamma_1}{3!}He_3(x) + \frac{\gamma_2}{4!}He_4(x)\right]e^{-\frac{x^2}{2}}, \\ x &= \frac{p-\mu}{\sigma}, \end{aligned} \tag{10}$$

with He_i being the ith probabilists' Hermite polynomial, μ and σ being the mean and standard deviation of the momentum, and γ_1, γ_2 being the cumulants due to skew and kurtosis, respectively. Since $He_0(x) = 1, I_{src}(p)$ collapses into a Gaussian function for $\gamma_1 = \gamma_2 = 0$. This form was chosen since the mean momentum can easily be converted into a mean velocity, and according to Ref. 12, a single temperature plasma should very closely be described by a Gaussian in neutron momentum.

To test this method, a highly distorted simulation of a NIF implosion was used to obtain neutron spectra along the individual LoS where the nToF detectors are located. These spectra were fit with the above described formalism, and the obtained matrix M was inverted to determine the hot spot velocity vector and then compared to the actual input value of the simulation. To determine the influence of skew and kurtosis on the deduced vector, this was done twice: once with the γ_1 and γ_2 parameters forced to zero and once with them included in the χ^2 minimization of the fit. Even though in this case those parameters were inconsistent with a zero value, the deduced velocity vector did not change significantly. Table I summarizes the obtained velocity vector and Fig. 3 shows a typical fit for a simulated spectrum.

TABLE I. Velocity vector results for a distorted simulation compared to the simulation input. Uncertainties quoted were taken from the fit uncertainty.

Quantity	Gauss only	With skew and kurtosis	Simulated value
Velocity magnitude (km/s)	126 ± 1	128 ± 1	120
θ (deg)	96 ± 5	95 ± 5	111
ϕ (deg)	313 ± 7	313 ± 7	319

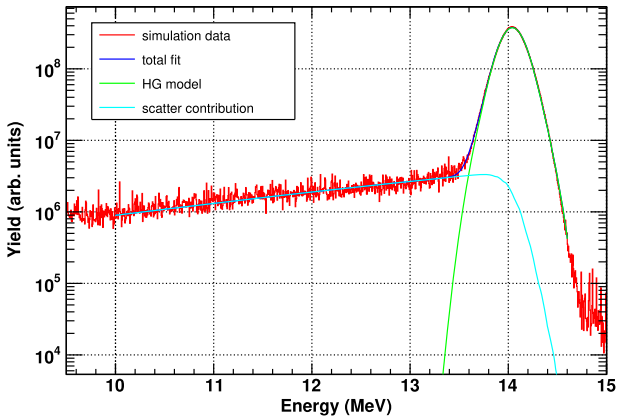

FIG. 3. Example fit of the Hermite Gauss (HG) model given by Eq. (10) to a distorted simulation.

Although the values in Table I do not exactly agree with the simulated values, actual uncertainties on an nToF measurement are considerably larger. A possible contribution to this discrepancy could be attributed to the scattering model (described in Ref. 9) which assumes only single scatter on an infinitesimal thin spherical shell of ρR of the DT ice.

IV. COMPARING RESULTS AND CONCLUSIONS

Several NIF shots have been analyzed with both the single LoS method that relies on the temperature model and the multi LoS analysis which calculates the hot spot velocity vector and the mean velocity of the neutron in the hot spot frame from a single matrix inversion. To compare the results of the two methods, the hot spot velocity vector obtained by the multi LoS analysis was projected onto each LoS and then compared with the result of each single LoS measurement. In almost all cases, results were consistent within the experimental uncertainties (see Fig. 4). For the experimental data analysis, the uncertainties are almost entirely systematical and come largely from

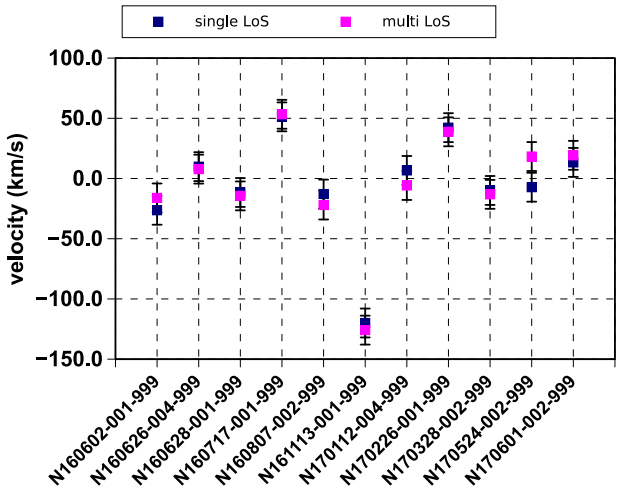

FIG. 4. Comparing the velocities obtained along the north pole LoS with the two different methods.

the uncertainty of the absolute timing: the reported bang time has an uncertainty of 40 ps–50 ps, and establishing the time offset on the photo diode scope channel has an uncertainty of ≈90 ps due to the need to cross calibrate it with a PMT. This gives a total timing uncertainty of ≈100 ps, which equates to a velocity uncertainty at 20 m of ≈13 km/s. By contrast, an uncertainty of 1 mm in the distance would correspond to 2.6 km/s and is therefore negligibly small.

Additionally it is possible to use the value of $\langle v \rangle$ to calculate the mean energy of the emitted neutrons, which can be converted to an ion temperature using the inverse of Eq. (4). This method of determining the ion temperature has the advantage of being independent of plasma flows; however, the current velocity uncertainty of 13 km/s leads to a temperature uncertainty of 1.1 keV. Using this method, the temperature has been computed for the set of shots for which the velocities were compared. The data comparing this temperature deduction to the ion temperatures obtained from the neutron peak width are shown in Fig. 5. Most temperatures seem to be in agreement within the quoted uncertainties.

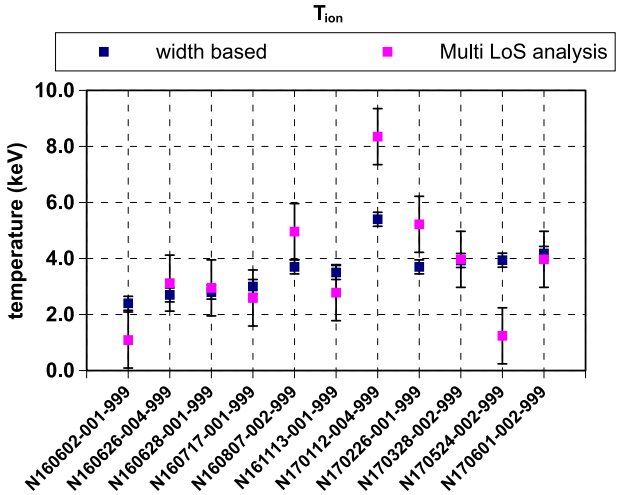

FIG. 5. Comparing neutron peak variance based ion temperatures with those obtained with the multi LoS velocity analysis.

V. SUMMARY

Two different methods to diagnose hot spot motion using nToF detectors have been developed and compared with each other. One method uses the model prescribed by Ballabio *et al.*[5] to estimate the mean energy of the neutron peak on a temperature derived from the variance of the neutron peak to determine the projection of the hot spot motion onto the LoS of the detector; the other method uses an ensemble of at least four detectors to obtain the hot spot velocity vector as well as the mean energy of the neutron peak via a matrix inversion. Both of these methods have advantages and disadvantages: the disadvantage of the single LoS analysis is the need for a model to relate the ion temperature to the mean energy of the neutron peak and the question of which "temperature" to use in this model. The advantage that this method has over the multiple LoS analysis method is that it will give information even if less than all four nToF detectors deliver reliable data. The multiple LoS analysis also provides another way of inferring ion temperature from nToF data; however, with the current setup, the timing uncertainty imposes an error bar slightly above 1 keV. Future work should address improving the timing uncertainties and apply these methods to the Cherenkov detector analysis.[7]

ACKNOWLEDGMENTS

This work was performed under the auspices of the U.S. Department of Energy by Lawrence Livermore National Laboratory under Contract No. DE-AC52-07NA27344.

[1]J. D. Lindl, L. J. Atherton, P. A. Amednt, S. Batha, P. Bell, R. L. Berger, R. Betti, D. L. Bleuel, T. R. Boehly, D. K. Bradley, D. G. Braun, D. A. Callahan, P. M. Celliers, C. J. Cerjan, D. S. Clark, G. W. Collins, R. C. Cook, E. L. Dewald, L. Divol, S. N. Dixit, E. Dzenitis, M. J. Edwards, J. E. Fair, R. J. Fortner, J. A. Frenje, V. Y. Glebov, S. H. Glenzer, G. Grim, S. W. Haan, A. V. Hamza, B. A. Hammel, D. R. Harding, S. P. Hatchett, C. A. Haynam, H. W. Herrmann, M. C. Herrmann, D. G. Hicks, D. E. Hinkel, D. D. Ho, N. Hoffman, H. Huang, N. Izumi, B. Jacoby, O. S. Jones, D. H. Kalantar, R. Kauffman, J. D. Kilkenny, R. K. Kirkwood, J. L. Kline, J. P. Knauer, J. A. Koch, B. J. Kozioziemski, G. A. Kyrala, K. L. Fortune, O. L. Landen, D. Larson, R. Lerche, S. L. Pape, R. London, B. J. MacGowan, A. J. MacKinnon, T. N. Malsbury, E. R. Mapoles, M. M. Marinak, P. W. McKenty, N. Meezan, D. D. Meyerhofer, P. Michel, J. Milovich, J. D. Moody, M. Moran, K. A. Moreno, E. I. Moses, D. H. Munro, A. Nikroo, R. E. Olson, T. Parham, R. W. Patterson, K. Peterson, R. Petrasso, S. M. Pollaine, J. E. Ralph, S. P. Regan, H. F. Robey, M. D. Rosen, R. Sacks, J. D. Salmonson, T. C. Sangster, S. M. Sepke, D. H. Schneider, M. B. Schneider, M. Shaw, B. K. Spears, P. T. Springer, C. Stoeckl, L. J. Suter, C. A. Thomas, R. Tommasini, R. P. Town, B. M. VanWonterghem, R. Vesey, S. V. Weber, P. J. Wegner, K. Widman, C. C. Widmayer, M. Wilke, H. L. Wilkens, E. A. Williams, D. C. Wilson, and B. K. Young, Nucl. Fusion **51**, 094024 (2011).

[2]M. J. Edwards, P. K. Patel, J. D. Lindl, L. J. Atherton, S. H. Glenzer, S. W. Haan, J. D. Kilkenny, O. L. Landen, E. I. Moses, A. Nikroo, R. Petrasso, T. C. Sangster, P. T. Springer, S. Batha, R. Benedetti, L. Bernstein, R. Betti, D. L. Bleuel, T. R. Boehly, D. K. Bradley, J. A. Caggiano, D. A. Callahan, P. M. Celliers, C. J. Cerjan, K. C. Chen, D. S. Clark, G. W. Collins, E. L. Dewald, L. Divol, S. Dixit, T. Doeppner, D. H. Edgell, J. E. Fair, M. Farrell, R. J. Fortner, J. Frenje, M. G. G. Johnson, E. Giraldez, V. Y. Glebov, G. Grim, B. A. Hammel, A. V. Hamza, D. R. Harding, S. P. Hatchett, N. Hein, H. W. Herrmann, D. Hicks, D. E. Hinkel, M. Hoppe, W. W. Hsing, N. Izumi, B. Jacoby, O. S. Jones, D. Kalantar, R. Kauffman, J. L. Kline, J. P. Knauer, J. A. Koch, B. J. Kozioziemski, G. Kyrala, K. N. LaFortune, S. L. Pape, R. J. Leeper, R. Lerche, T. Ma, B. J. MacGowan, A. J. MacKinnon, A. Macphee, E. R. Mapoles, M. M. Marinak, M. Mauldin, P. W. McKenty,

M. Meezan, P. A. Michel, J. Milovich, J. D. Moody, M. Moran, D. H. Munro, C. L. Olson, K. Opachich, A. E. Pak, T. Parham, H.-S. Park, J. E. Ralph, S. P. Regan, B. Remington, H. Rinderknecht, H. F. Robey, M. Rosen, S. Ross, J. D. Salmonson, J. Sater, D. H. Schneider, F. H. Séguin, S. M. Sepke, D. A. Shaughnessy, V. A. Smalyuk, B. K. Spears, C. Stoeckl, W. Stoeffl, L. Suter, C. A. Thomas, R. Tommasini, R. P. Town, S. V. Weber, P. J. Wegner, K. Widman, M. Wilke, D. C. Wilson, C. B. Yeamans, and A. Zylstra, Phys. Plasmas **20**, 070501 (2013).

[3]A. L. Kritcher, R. Town, D. Bradley, D. Clark, B. Spears, O. Jones, S. Haan, P. T. Springer, J. Lindl, R. H. H. Scott, D. Callahan, M. J. Edwards, and O. L. Landen, Phys. Plasmas **21**, 042708 (2014).

[4]M. G. Johnson, J. A. Frenje, D. T. Casey, C. K. Li, F. H. Séguin, R. Petrasso, R. Ashabranner, R. M. Bionta, D. L. Bleuel, E. J. Bond, J. A. Caggiano, A. Carpenter, C. J. Cerjan, T. J. Clancy, T. Doeppner, M. J. Eckart, M. J. Edwards, S. Friedrich, S. H. Glenzer, S. W. Haan, E. P. Hartouni, R. Hatarik, S. P. Hatchett, O. S. Jones, G. Kyrala, S. L. Pape, R. A. Lerche, O. L. Landen, T. Ma, A. J. MacKinnon, M. A. McKernan, M. J. Moran, E. Moses, D. H. Munro, J. McNaney, H. S. Park, J. Ralph, B. Remington, J. R. Rygg, S. M. Sepke, V. Smalyuk, B. Spears, P. T. Springer, C. B. Yeamans, M. Farrell, D. Jasion, J. D. Kilkenny, A. Nikroo, R. Paguio, J. P. Knauer, V. Y. Glebov, T. C. Sangster, R. Betti, C. Stoeckl, J. Magoon, M. J. Shoup III, G. P. Grim, J. Kline, G. L. Morgan, T. J. Murphy, R. J. Leeper, C. L. Ruiz, G. W. Cooper, and A. J. Nelson, Rev. Sci. Instrum. **83**, 10D308 (2012).

[5]L. Ballabio, J. Källne, and G. Gorini, Nucl. Fusion **38**, 1723 (1998).

[6]T. J. Clancy, J. Caggiano, J. McNaney, M. Eckart, M. Moran, V. Y. Glebov, J. Knauer, R. Hatarik, S. Friedrich, R. Zacharias, A. Carpenter, M. J. Shoup, T. Buczek, M. Yeoman, Z. Zeid, N. Zaitseva, B. Talison, J. Worden, B. Rice, T. Duffy, A. Pruyne, and K. Marshall, Proc. SPIE **9211**, 92110A (2014).

[7]A. S. Moore, D. J. Schlossberg, E. P. Hartouni, D. Sayre, M. J. Eckart, R. Hatarik, F. Barbosa, J. Root, C. Waltz, B. Beeman, M. S. Rubery, and G. P. Grim, Rev. Sci. Instrum. **89**, 10I120 (2018).

[8]E. P. Hartouni, B. Beeman, M. J. Eckart, G. P. Grim, R. Hatarik, A. S. Moore, M. Rubery, D. Sayre, D. J. Schlossberg, and C. Waltz, "Uncertainty analysis of response functions and γ-backgrounds on T_{ion} and t_0 measurements from Cherenkov neutron detectors at the National Ignition Facility (NIF)," Rev. Sci. Instrum. (these proceedings).

[9]R. Hatarik, D. B. Sayre, J. A. Caggiano, T. Phillips, M. J. Eckart, E. J. Bond, C. Cerjan, G. P. Grim, E. P. Hartouni, J. P. Knauer, J. M. Mcnaney, and D. H. Munro, J. Appl. Phys. **118**, 184502 (2015).

[10]T. J. Murphy, Phys. Plasmas **21**, 072701 (2014).

[11]H. W. Herrmann, N. Hoffman, D. C. Wilson, W. Stoeffl, L. Dauffy, Y. H. Kim, A. McEvoy, C. S. Young, J. M. Mack, C. J. Horsfield, M. Rubery, E. K. Miller, and Z. A. Ali, Rev. Sci. Instrum. **81**, 10D333 (2010).

[12]D. H. Munro, Nucl. Fusion **56**, 036001 (2016).